Bulgarian Chemical Communications, Volume 58, Issue 4 (pp. 515-522) 2026 *DOI: 10.34049/bcc.58.4.5759*

Parametric optimization of ZK60 reinforced with ZrB_2 magnesium composites *via* Taguchi method

S. Suresh Kumar[1,2*], V. Mohanavel [3]

[*1]*Department of Mechanical Engineering, Bharath Institute of Higher Education and Research, Selaiyur, Chennai 600073, Tamil Nadu, India*

[2]*Department of Mechanical Engineering, PERI Institute of Technology, Mannivakkam, Chennai 600048, Tamil Nadu, India*

[3]*Centre for Sustainable Materials Research, Department of Mechanical Engineering, Academy of Maritime Education and Training (AMET), Deemed to be University, Kanathur, Chennai 603112, Tamil Nadu, India*

Received: April 17, 2026; Revised: June 17, 2026

The exploit of composite materials in many industrial usages is growing. By selecting the right materials, the composite could be customized to meet specific necessities as per suggestion of an engineer. Magnesium metal matrix composites (MMMCs) are a superior replacement for conventional alloys. By using the liquid metallurgy stir casting (SC) route to reinforce ZK60 with zirconium diboride (ZrB_2) particles, MMMCs were created. This study investigates the effect of ZrB_2 reinforcement (0, 4, 8 and 12) wt % (C1) on the wear and corrosion properties of composites produced. The wear examination was conducted at 20 N applied load (C2), 4 m/s sliding velocity (C3), 1500 m sliding distance (C4), 478 rpm speed for 1500 s. The variation of the wear loss in g for the different reinforcements was determined. The corrosion rate was determined using salt spray analysis. The wear and corrosion results showed that the 12 wt.% composite samples had lower wear loss and corrosion rate than those of ZK60 alloy. Furthermore, the Taguchi optimization process was adopted to investigate the parametric impact on the wear rate (WR), including C1, C2, C3 and C4. The primary effect plot shows that the least WR is achieved at 12 wt.% of ZrB_2 (C1), 5 N C2, 4 m/s C3, and 750 m C4. C1 is a notable variable for getting the least WR, with an impact of 43.34%, and next to it is C4 (21.21% impact). The factors C2 and C3 have smaller impacts according to the analysis of variance (ANOVA) data.

Keywords: ZK60, ZrB_2, stir casting, wear, Taguchi, optimization

INTRODUCTION

Composites are devised by blending multiple constituents that are exclusive in terms of material composition and properties. The two constituents that are most notable for their insoluble nature are the matrix and the reinforcing phase during the composite manufacturing process. The reinforcing phase often possesses higher degrees of strength and hardness than the matrix phase. The matrix materials and the reinforcing types, devised in the creation of composites, are the fundamental factors that determine the classification of these materials into a variety of distinct categories. The world's mechanical component manufacturing businesses are shifting toward the use of composites to cut weight without sacrificing the properties of the material [1, 2].

A combination of the material's own distinctive characteristics has been produced as a consequence of interaction. When mixed with different types of reinforcement materials, this unique material combination offers certain desirable qualities. It is widely employed in many different industries, including the maritime, automotive, and aerospace sectors.

The composite material can combine the most desirable properties of its components whilst suppressing less advantageous properties; this allows the composite material to display exclusive mechanical and physical properties. The creation of innovative materials and the deeper perception of the association between structure and qualities of the materials results in the development of novel composites [3, 4]. Metal matrix composites (MMCs) can be designed with desired properties by varying the type, shape, volume %, and distribution of ceramic reinforcing phases added to a metal matrix. Combining two or more materials that together have better qualities than either material alone yields metal-metal composites. Either a metal or an alloy based on metal makes up the matrix of this composite material. On the other hand, the majority of ceramics used for reinforcement are whiskers and particulates.

In order to meet the demanding and competitive quirements for particular material attributes, and the obsolescence of high-strength, lightweight

* To whom all correspondence should be sent: Email: *sandysureesh@gmail.com*

© 2026 Bulgarian Academy of Sciences, Union of Chemists in Bulgaria

materials, modern businesses are creating innovative manufacturing processes for reinforcing materials.

In this respect, MMCs are materials with good strength and low weight that are produced by a diversity of technical routes, including processing in liquid, solid, and vapor states. MMCs perform better than monolithic materials with respect to wear strength, stiffness, thermal conductivity and creep opposition [5, 6]. MMCs have improved qualities like wear resistance, tensile strength at room temperature and higher temperatures, hardness, and elastic modulus, together with important weight reserves over unreinforced metals. They are finding increased employment in airspace and automotive industries. Because of their special properties, MMCs have potential uses in a variety of contexts. These materials were created in response to the market need for materials with high levels of stiffness, wear resistance, and strength [7, 8].

Over the last few decades, there has been a rise in the use of magnesium in numerous distinct applications. This is because magnesium is the lightest metal and can replace aluminum. Magnesium is also capable of being used for a variety of other purposes. Owing to their exceptional cast ability, high stiffness, and strength, magnesium alloys are lightweight materials with diversified commercial applications. They have a high rate of recycling, are better at absorbing vibrations than steel and aluminum, are lighter and machine-friendly. They also provide a good substitute material for parts used in automobiles and aircraft. Light metals like magnesium are commonly utilized as the matrix in structural applications, providing strong support for the reinforcement. The matrix is implanted with the reinforcing substance. In addition to its primary function of reinforcing the material, reinforcement can also be utilized to modify physical qualities including wear opposition, friction coefficient, and thermal conductivity [9, 10].

Magnesium is less dense than typical metals, has better mechanical properties, is more resistant to corrosion and wear, and exhibits a lower thermal coefficient of expansion while mapped to customary materials. These days, more people are becoming aware of Mg and its alloys due to their good strength-to-weight ratio and low density. Because of their appealing biodegradation and mechanical qualities, Mg alloys and composites are employed as typical materials and have been regarded as viable alternatives of numerous alloys [11].

MMCs are a novel type of composites that are extensively used in the transportation sectors due to their lower density, greater mechanical properties, augmented opposition to corrosion and wear, compared to traditional metals and alloys. MMCs are interesting because, after being reinforced with metals and ceramics, they play a major role in a variety of lightweight applications. Over the last few decades, different efficient processes have been expanded to produce MMCs with uniformly dispersed reinforcements and strong interfacial bonding, ultimately leading to better performance [12, 13]. By incorporating several types of reinforcement, magnesium-matrix composites have been created to enhance the wear opposition of magnesium and its alloys. For many engineering applications, these MMMCs are the ideal option [14, 15]. Zirconium diboride (ZrB_2) is a member of the ultrahigh temperature ceramics material class. owing to its strong thermal and electrical conductivities, as well as its high melting temperature (over 3000 °C) [16, 17]. ZrB_2 is a great option for applications in harsh settings including elevated temperature electrodes, thermal guard systems and molten metal crucibles because of its unique set of characteristics. When set against alternative non-oxide structural ceramics, ZrB_2 has a good melting point, high strength, low density, and outstanding resistance to thermal shock and oxidation [18, 19].

For MMCs, a broad variety of manufacturing processes, both liquid-state and solid-state, have been studied. A multitude of processes, including squeeze casting, vapor deposition, stir casting, and powder metallurgy, have been developed to create MMCs. When compared to other fabrication techniques, stir casting is superior since it is simpler and can produce large quantities of composites. The stir cast (SC) fabrication route has numerous gains over other routes including accessibility, compliance, resourcefulness with other materials, and an inexpensive, elevated manufacture rate [20, 21]. The SC route is the most utilized commercial fabrication route because of its unique characteristics. SC creates MMCs by incorporating metallic or ceramic powders into a desired matrix. In SC, the powders are supplemented to the molten mix in a crucible and then agitated to achieve a fine circulation of the powders in the matrix.

The process creates a vortex in the liquid metal by means of a stirring mechanism. The easy integration of the particles with the few available types of stirring devices leads to a uniform dispersion. Stir casting has gained popularity because of its affordability, effortlessness of usage,

and capability to produce big quantities [22, 23]. When compared to other manufacturing methods, the SC process is simple to use, inexpensive, and appropriate for large-scale manufacture. The severe distortion during extrusion creates a very fine microstructure that improves the mechanical strength and hardness of the specimens. The increase in hardness is thought to be caused by adding harder granules to the structure, making it easier for grain boundaries to separate, and setting the ceramic particles out evenly [24, 25]. In mechanical terms, increasing the TiN content enhances the component's hardness and strength. At 12 wt % of TiN, the attained strength of the composites is 160 MPa and 80 HV. In salt spray and electrochemical assessments, elevated TiN amounts mitigated corrosion and mass loss. 12 wt.% of TiN offered the highest level of resistance [26]. New AZ91D/ZrB_2 composite study improved its mechanical characteristics. The addition of ZrB_2 particles to the AZ91D demonstrated favorable resultsthe composites is compared to earlier studies. This study produced AZ91D/ZrB_2 with different reinforcement weights using squeeze casting and AZ91D/12 wt.% by stir casting [27].

The authors of [28] optimized the influence of reinforcement weight percentages on the wear characteristics of Mg/TiC/MoS_2 composites and both reinforcements considerably enhanced the wear aversion of the produced composites compared to the Mg matrix. The authors of [29] analyzed the tribology parameters of Mg-3Al-5.6Ti composites and found that the inclusion of reinforcement particles enhances the wear resistance. The numerical examination of the wear behavior of Mg composites is reported in ref. [30]. In ref. [31] the wear parameter of Mg (5.6Ti+3Al)2.5 B_4C composites is studied. The authors of [32] explored the wear characteristics of AZ91E composites and determined that the conversion load increases as the amount of reinforcement enhances and the wear rate of the composite decreases relative to the alloy. The authors of [33] examined the wear characteristics of Mg armored with SiC. Under a lower load, the wear resistance of the composites is marginally better; however, at a higher load, the benefits of the SiC impregnation on wear are less clear. Girish *et al.* [34] probed the wear properties of AZ91-SiC-Gr composites and the findings demonstrate that, in the test conditions, the wear resistance of the composites was appreciably superior. The article [35] examined the wear behavior of TiC-, SiC- and fly ash-augmented Mg matrix and concluded that as the applied load rose, the wear rate and coefficient of friction increased for all samples. The research [36] explored the corrosion characteristics of Mg-SiC composites and found that the composites' SiC reinforcement and magnesium matrix did not considerably increase the rate of corrosion overall. The research [37] investigated the wear behavior of Mg-SiC-Gr composites and reported that because of the upright effect provided by both reinforcements, the resulting composites' wear resistance improved considerably more than the magnesium matrices. Amid the fabricated composites, the 5wt.% Gr-strengthened Mg-10SiC composites have good wear resistance.

The authors of [38] examined the corrosion and wear characteristics of a ZK60-10HA (hydroxyapatite) composite and stated that according to the findings, magnesium matrix composites that are biocompatible can effectively prevent corrosion and wear by utilizing HA particles as an inhibitor. The goal of this endeavor was to improve the ZK60 resistance to corrosion and to make it more durable. This was accomplished by incorporating micro-SiC and nano-AlN as fortifications into the material. The corrosion properties of the extrudates on both surfaces were evaluated while the extrusion process was in operation [39]. There is an increasing claim for materials that are both lightweight and sturdy, and as a result, the potential for magnesium composites has expanded in multiple sectors. In current decades, there has been an increase in the scope of potential applications for magnesium [40].

A limited selection of the available literature that have been offered in recent times is included in this study, which focuses on the fusion of reinforcements with various magnesium. However, no studies on the effect of ZrB_2 on ZK60 have been studied. Also, there is insufficient information accessible on the properties of ZK60 composites. Thus, our aim is to study the consequences of varying ZrB_2 reinforcement on the wear, and corrosion properties of the ZK60 composites and to focus on the optimization of wear parameters (WR) of MMMCs synthesized through stir casting.

EXPERIMENTAL

ZrB_2 particles were employed in the present work as reinforcements in a ZK60 alloy matrix. Through SC method, composites with different degrees of reinforcement including 0, 4, 8, and 12 % were used to synthesize the ZK60/0 wt.% ZrB_2, ZK60/4 wt.% ZrB_2, ZK60/8 wt.% ZrB_2, and ZK60/12 wt.% ZrB_2 composites and the raw material and fabricated sample is shown in Figure 1.



Figure 1. Raw material and prepared composite

In order to produce the composite specimen, the stir casting procedure was applied. This is due to the fact that it ensures a more equal dispersion of the reinforcing particles across the entirety of the specimen. The utilization of this technique allows for the manufacture of composites that contain particles to be achieved at the most cost-effective level feasible. The matrix alloy or matrix material was initially heated to a temperature that was higher than its melting point. In order to keep the matrix alloy in a semisolid state, the temperature was gradually lowered to a level that was lower than the liquid condition. This was done in order to maintain the matrix alloy. As soon as the temperature reached this level, the warmed reinforcement particles, at predetermined weight percentage were added to the slurry, and a stirrer was used to blend the particles. As the temperature of the composite slurry was being raised to a completely molten state, stirring was maintained at an average stirring speed while an argon gas shield provided an inert atmosphere for protection [41]. The entire process of fabrication with the processing parameters is shown in a flow chart (Figure 2).

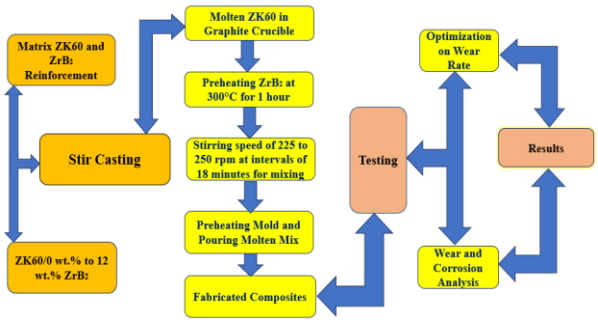


Figure 2. Entire work flow process of the research

The scheme of the casting setup is presented in Figure 3.

Initially, constants of 20 N (C2), 4 m/s (C3), and 1500 m (C4), sliding diameter of 40 mm, 478 rpm of sliding speed and 1500 s duration were used to conduct the wear test.

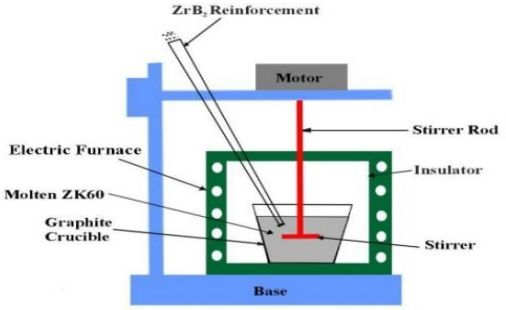


Figure 3. Scheme of the stir casting setup

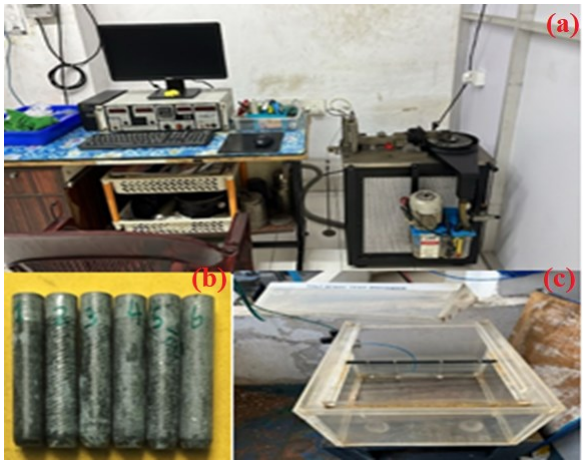


Figure 4. a) Wear tester (b) Wear sample (c) Salt spray

The wear tester is shown in Figure 4 (a). The machined samples are shown in Figure 4 (b). The salt spraying test is utilized and used weight loss methods to calculate the corrosion loss on composite samples with a size of 10×10×10 mm and the setup is shown in Figure 4 (c). It is carried out in compliance with ASTM B117. Wear examinations were performed utilizing the pin-on-disc (POD) tester on the composite specimens. As per ASTM G99, the specimens were made with size of 30 mm in length and 8 mm in diameter. Wear testing was performed at the room temperature at .

Taguchi's approach was applied to the experimentations. WR was considered as the output response in this study [42] and the four-level with four input components were chosen for experimentation which is displayed in Table 1.

Table 1. Parametric levels

Input parameters and their units	Levels			
	1	2	3	4
C1 (%)	0	4	8	12
C2 (N)	5	10	15	20
C3 (m/s)	1	2	3	4
C4 (m)	750	1000	1250	1500

RESULTS AND DISCUSSION

Wear analysis

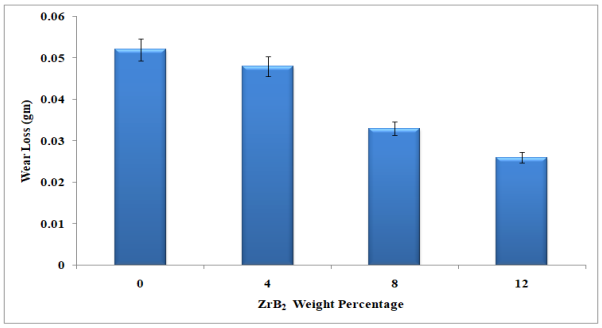


Figure 5. Weight percentage of reinforcement *vs.* wear loss

As seen in Figure 5, wear rate values fell as ZrB_2 weight percentage increased. The wear loss was significantly less than that of ZK60 alloy and ZK60/12wt.% ZrB_2 composites. Comparing the samples ZK60/8wt.% ZrB_2 and ZK60/4wt.%ZrB_2 to ZK60 alloy, a decrease in wear rate was also noted with a decline in values when reinforcement is increased. Nonetheless, the surface qualities are influenced by the weight fraction of the reinforcement.

Corrosion analysis

Figure 6 shows the weight loss for the ZK60 alloy, ZK60/4wt.% ZrB_2, ZK60/8wt.% ZrB_2, and ZK60/12wt.% ZrB_2 composite. The weight loss during the salt spray test is lessened by the increased ZrB_2 presence in the ZK60 alloy. When the wt.% of ZrB_2 added to the ZK60 matrix in increasing order, the corrosion rate also falls. For the fabricated composite samples, there is an improvement in corrosion resistance. This is because ZrB_2 is dispersed appropriately in the matrix's grain boundary, where it forms an appropriate passive layer that shields the surface from corrosion. It has been observed that raising the amounts of wt.% of particle in the ZK60 progressed the corrosion resistance.

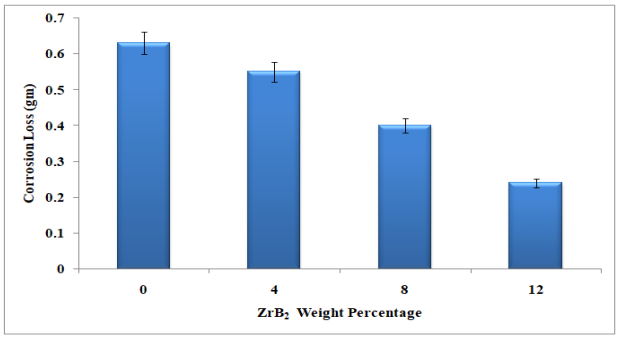


Figure 6. Weight percentage of reinforcement *vs.* corrosion loss.

Optimization for WR

Using a POD tester, produced ZK60/ZrB_2 composites' wear rate was assessed. The Taguchi approach [42] was utilized to optimize the variables for WR as optimization yields significant benefits, particularly in regard to cost savings. Industries may significantly minimize waste which greatly increases production. Since wear is an important parameter for any mechanical components this study is considered and the results are examined in as in Table 2.

Table 2. L_{16} orthogonal array

Exp. No	C1	C2	C3	C4	WR (mm^3/m)	S/N Ratio
1	0	5	1	750	0.044	27.1309
2	0	10	2	1000	0.047	26.5580
3	0	15	3	1250	0.050	26.0206
4	0	20	4	1500	0.053	25.5145
5	4	5	2	1250	0.044	27.1309
6	4	10	1	1500	0.053	25.5145
7	4	15	4	750	0.034	29.3704
8	4	20	3	1000	0.043	27.3306
9	8	5	3	1500	0.040	27.9588
10	8	10	4	1250	0.035	29.1186
11	8	15	1	1000	0.039	28.1787
12	8	20	2	750	0.034	29.3704
13	12	5	4	1000	0.021	33.5556
14	12	10	3	750	0.022	33.1515
15	12	15	2	1500	0.039	28.1787
16	12	20	1	1250	0.040	27.9588

Analysis of WR

Tables 3 and 4 display the WR - S/N ratio and WR mean for the produced ZK60/ZrB_2 composites. The tables show the response mean and the S/N ratio mean value for every intensity of control parameter. The arrangement of the important mechanism on the intended response value is demonstrated by a certain rank. Moreover, the tables demonstrate that the wt % of ZrB_2 particle (C1) has the biggest influence on WR, with the normal C4, C3, and C2 following in that order. This is explained by the ZrB_2 particles' contribution to the ZK60 composites which lowers the WR. Nonetheless, the wear rate is increased by C2. This is brought on by increased contact pressure between the disc surface and pin, which raises the WR.

Table 3. Response table for signal to noise of WR

Levels	C1	C2	C3	C4
1	-28.40	-29.20	-28.68	-29.45
2	-28.72	-29.08	-28.88	-29.18
3	-29.14	-28.92	-29.09	-28.80
4	-29.71	-28.79	-29.32	-28.55
Delta	1.31	0.41	0.64	0.90
Rank	1	4	3	2

Table 4. Response table for means

Levels	C1	C2	C3	C4
1	26.31	28.94	27.20	29.76
2	27.34	28.59	27.81	28.91
3	28.66	27.94	28.62	27.56
4	30.71	27.54	29.39	26.79
Delta	4.41	1.40	2.19	2.96
Rank	1	4	3	2

Figures 7 and 8 display the primary influence of WR through the S/N ratio and the mean value. The ideal level of each component and each one's impact on the WR of the tested ZK60/ZrB_2 composites are visible from the graphs. Figure 7 shows that the optimum levels of the following factors (12 wt.%), C2 (5 N), C3 (4 m/s), and C4 (750 m)—achieve the lowest WR. Figure 7 also makes it evident that as the weight percentage of ZrB_2 material is added, the WR steadily decreases.

The ZK60 composites reinforced with 12 wt.% ZrB_2 particles exhibit the lowest WR value of 0.021 mm3/m. It is evident that the WR increases in accordance with the Archard's law as the load increases. WR for the sliding velocity is largest at inferior speeds and diminishes with escalating speed. About the C4, more surface contact leads to a higher localized temperature, which in turn causes more metal loss. Therefore, as the sliding distance increases, so does the WR.

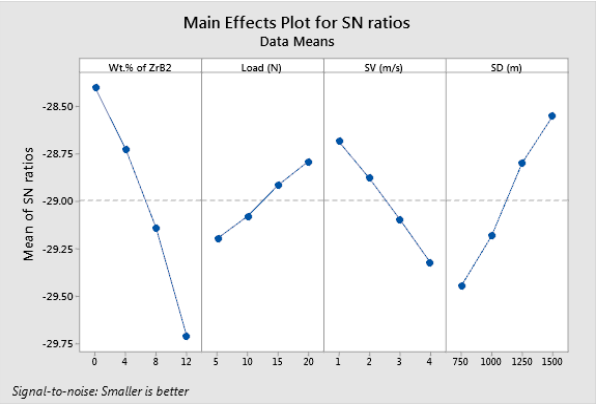


Figure 7. Main effects plot for S/N ratio of WR

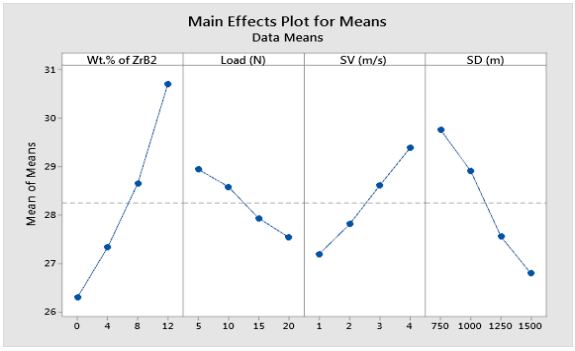


Figure 8. Main effects plot for means of WR

Contour plot analysis

The wear rate of ZK60/ZrB_2 composite is analyzed in Figure 9 (a–d) *via* contour plot analysis. Figure 9 (a) displays the WR of C1 *vs*. C2, Figure 9 (b) displays the WR of C2 *vs*. C3, Figure 9 (c) displays the WR of C3 *vs*. C4, Figure 9 (d) displays the WR of C1 *vs*. C4. It is evident from these plots that the weight percentage of ZrB_2 has a greater influence on the WR of the fabricated composites. However, a raise in load causes material wear because of the high contact pressure. This is because it is evident from the essentials of tribology that an augment in C4 results in an increase in wear volume, but the WR remains nearly constant. Overall, the contour plot analysis identifies the parameter regions that provide optimal and stable operating conditions, thereby facilitating process optimization and enhancing the robustness of the tribological performance.

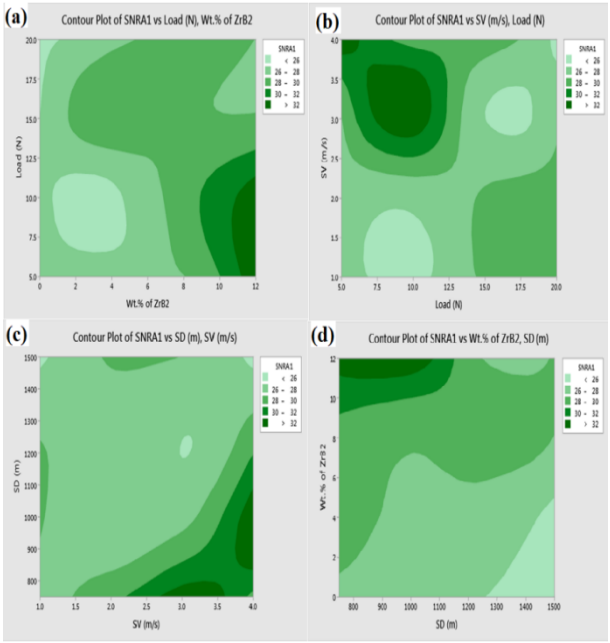


Figure 9. Contour plot for WR of (a) C1 *vs*. C2, (b) C2 *vs*. C3 (c) C3 *vs*. C4 (d) C1 *vs*. C4

Analysis of variance

ANOVA is an arithmetical design tool with an emphasis on least squares that is widely used to separate the individual effects from each of the control components. It is used to establish the order of factors in this study at a significance level of 5%. If a factor's P-value is less than 0.05, it is confirmed that the variables have an empirically noteworthy influence on the responses. Table 5 presents the WR of the ZK60/ZrB_2 composites that were created, as determined by an ANOVA and it could be witnessed that the P-values for C1 and C4 are less than 0.05, signifying that overall parameters encompass an important influence on WR. Moreover, the involvement of C1 had an effect of 43.34% and C4 had an effect of 21.21% on WR of the produced composites.

Table 5. ANOVA for WR

Source	DF	Adj SS	Adj MS	F-value	P-value
C1	3	43.344	14.4480	29.10	0.010
C2	3	4.765	1.5884	3.20	0.183
C3	3	10.952	3.6508	7.35	0.068
C4	3	21.217	7.0724	14.24	0.028
Error	3	1.490	0.4965		
Total	15	81.768			

CONCLUSIONS

In the current work MMCs are successfully synthesized using a stir casting method with different weight percentages of ZrB_2 particles (0, 4, 8, and 12 wt.%). This work focuses on the wear and corrosion properties of ZK60/ZrB_2 strengthened with various weight percentages of ZrB_2. Simultaneously, the ZK60/ZrB_2 underwent wear testing using a POD setup for finding the minimal wear rate in determining optimal parameter. The ZK60 alloy's wear and corrosion resistance significantly improved upon the addition of ZrB_2 particles up to a weight percentage of 12. The ZK60 alloy matrix composite containing 12 weight percent ZrB_2 showed excellent corrosion resistance, with corrosion loss of 0.242 gm. The Taguchi technique was used to identify the ideal parameters for the developed composites' wear rate in dry sliding circumstances, and their impact on the wear rate is assessed. The S/N ratio graph indicates that the ideal dry sliding parameters for the developed composites are 12 weight percent of ZrB_2 content, 5 N C2, 4 m/s C3, and 750 m C4. These values result in the least WR of 0.021 mm^3/m. According to the results of the ANOVA, the weight percentage of ZrB_2 content has a significant impact on wear rate, contributing 43.34% of the total.

Acknowledgement: *Not applicable.*
Author contributions: *S. Suresh Kumar has done the original draft, reviewing and editing. V. Mohanavel has supervised the research work.*
Conflict of interest: *On behalf of the authors, the corresponding author states that there is no conflict of interest.*
Research funding: *Not applicable.*
Data availability: *Not applicable.*

REFERENCES

1. P. Bharathi, T. Sampath Kumar, *Proc. Inst. Mech. Eng. Part E: J. Process Mech. Eng*., **237**, 1014 (2023).
2. M. P. Reddy, N. Alsaleh, S. Ataya, K. R. Gopal, A. M. A. Mohamed, *J. Mater. Res. Technol*., **39**, 8076 (2025).
3. S. Seetharaman, J. Subramanian, R. A. Singh, W. L. E. Wong, M. L. S. Nai, M. Gupta, *Technologies*, **10**, 32 (2022).
4. D. K. Ammisetti, S. H. Kruthiventi, S.Vinjavarapu, N. N.,Babu, J. R. Gandepudi, S. K. Battula, *J. Eng. Appl. Sci*., **71,** 60 (2024).
5. P. K. Gupta, A. K. Trivedi, M. K. Gupta, M. Dixit, *Proc. Inst. Mech. Eng. Part L: J. Mater. Des. Appl.,* **238,** 1827 (2024).
6. K. Pooja, N. Tarannum, P. Chaudhary, *Discov. Mater*., **5**, 35 (2025).
7. S. Jhamb, J. Matai, J. Marwaha, A. Goyal, A. Pandey, *Adv. Mater. Process. Technol*., **9**, 1249 (2023).
8. N. Gupta, M. Paramsothy, *JOM*, **66**, 862 (2014).
9. P. Emadi, B. Andilab, C. Ravindran, *J. Indian Inst. Sci.*, **102**, 405 (2022).
10. J. Tan, S. Ramakrishna, *Appl. Sci.,* **11**, 6861 (2021).
11. Y. Yang, X. Xiong, J. Chen, X. Peng, D. Chen, F. Pan, *J. Magnesium Alloys*, **9**, 705 (2021).
12. V. K. Bommala, M. G. Krishna, C. T. Rao, *J. Magnesium Alloys*, **7,** 72 (2019).
13. V. K. Murali, M. S. Starvin, *J. Chil. Chem. Soc*., **68**, 5911 (2023).
14. S. K. Rohit Singh, D. Tiwari, S. Sahu, V. B. Jadhav, A. K. Jain, K. K. Pandey, *Lect. Notes Mech. Eng., ICRAM 2025, Recent Adv. Mater. Manuf. Sci*., 2025.
15. J. Y. Ren, G. C. Ji, H. R. Guo, Y. M. Zhou, X. Tan, W. F. Zheng, Q. C. Jiang, *Materials*, **17**, 2454 (2024).
16. N. Mustafa, N. N. A. Basir, R. E. Ibrahim, M. M. Mahat, N. N. Bonia, M. Y. Sabrina, R. Rosmamuahamadani, *Int. J. Eng. Technol*., **7**, 406 (2019).
17. E. W. Neuman, M. Thompson, W. G. Fahrenholtz, G. E. Hilmas, *J. Eur. Ceram. Soc*., **42**, 4024 (2022).
18. H. Wang, C. A. Wang, X. Yao, D. Fang, *J. Am. Ceram. Soc*., **90**, 1992 (2007).
19. J. K. Sonber, A. K. Suri, *Adv. Appl. Ceram*., **110**, 321 (2011).

20. P. Sarmah, K. Gupta, *Materials*, **17**, 4635 (2024).
21. D. Srinivasan, M. Meignanamoorthy, A. Gacem, M. Vinayagam, T. Sathish, M. Ravichandran, H. L. Allasi, *J. Nanomater*., **2022**, 7840939 (2022).
22. K. Shivalingaiah, V. Nagarajaiah, C. P. Selvan, S. T. Kariappa, N. G. Chandrashekarappa, A. Lakshmikanthan, E. Linul, *Metals*, **12**, 1297 (2022).
23. R. S. Martins, I. Zimpel, V. K. De Barcellos, *Mater. Today Commun*., **43**, 111718 (2025).
24. C. Morsiya, S. Pandya, *Arch. Metall. Mater*., **68,** 1473 (2023).
25. A. Kumar, S. Kumar, N. K. Mukhopadhyay, *J. Magnesium Alloys*, **6**, 245 (2018).
26. H. Saravanan, D. Veeman, D. Srinivasan, M. Ravichandran, *Ceram. Int*., **51**, 7130 (2025).
27. S. Ayyanar, A. Gnanavelbabu, K. Rajkumar, P. Loganathan, K. Vishal, Proc. *Inst. Mech. Eng. Part C: J. Mech. Eng. Sci.*, **237**, 692 (2023).
28. N. Selvakumar, P. Narayanasamy, *Tribol. Trans*., **59**, 733 (2016).
29. S. Sathish, V. Anandakrishnan, S. Sankaranarayanan, M. Gupta, *J. Tribol*., **23**, 76 (2019).
30. M. S. Lee, C. G. Kang, J. S. S. Babu, *Metals*, **13**, 1418 (2023).
31. S. Sathish, V. Anandakrishnan, M. Gupta, *Ind. Lubr. Tribol*., **72**, 503 (2019).
32 C. Tarasasanka, K. Snehita, K. Ravindra, D. Sameerkumar, *Int. J. Eng. Sci. Technol*., **11**, 41 (2019).
33 C. Y. H. Lim, S. C. Lim, M. Gupta, *Wear*, **255**, 629 (2003).
34 B. M. Girish, B. M. Satish, S. Sarapure, D. R. Somashekar Basawaraj, *Tribol. Trans*., **58**, 481 (2015).
35 A. Singh, N. Bala, *Mater. Res. Express*, **6**, 1065H1 (2019).
36 S. Tiwari, R. Balasubramaniam, M. Gupta, *Corros. Sci*., **49**, 711 (2007).
37 K. S. Prakash, P. Balasundar, S. Nagaraja, P. M. Gopal, V. Kavimani, *J. Magnesium Alloys*, **4**, 197 (2016).
38 J. Su, J. Teng, Z. Xu, Y. Li, *Friction*, **10**, 31 (2022).
39 A. Sager, I. Esen, H. Ahlatçi, Y. Turen, *Materials*, **15**, 8582 (2022).
40 K. Chauhan, J. Karloopia, R. S. Walia, M. Dhanda, *Crit. Rev. Solid State Mater. Sci.,* **49**, 1 (2024).
41 S. S. Kumar, V. Mohanavel, *Matéria (Rio de Janeiro*), **29**, e20240264 (2024).
42 S. S. Kumar, V. Mohanavel, *Interactions*, **245**, 208 (2024).